

Bulk flow scaling for turbulent channel and pipe flows

Xi Chen,^{1,2} Fazle Hussain,² and Zhen-Su She^{1,*}

¹State Key Laboratory for Turbulence and Complex Systems and Department of Mechanics,
College of Engineering, Peking University, Beijing 100871, China

²Department of Mechanical Engineering, Texas Tech University, Lubbock, Texas, 79409-1021, USA
(Dated: December 27, 2017)

We report a theory deriving bulk flow scaling for canonical wall-bounded flows. The theory accounts for the symmetries of boundary geometry (flat plate channel versus circular pipe) by a variational calculation for a large-scale energy length, which characterizes its bulk flow scaling by a simple exponent, i.e. $m = 4$ for channel and 5 for pipe. The predicted mean velocity shows excellent agreement with several dozen sets of quality empirical data for a wide range of the Reynolds number (Re), with a universal bulk flow constant $\kappa \approx 0.45$. Predictions for dissipation and turbulent transport in the bulk flow are also given, awaiting data verification.

PACS numbers: 47.27.eb, 47.27.nd, 47.27.nf

An intriguing feature of practical turbulent flows is the presence of net spatial momentum and energy transports, which are constrained by boundaries [1, 2]. Flows at the surface of a vessel or inside a pipeline, over the wings of an aircraft or close to the ground on windfarms, etc., develop abundant flow structures contributing to turbulent transports. However, even for canonical cases, i.e. flat-plate channels and cylinder pipes, the boundary effect has not been treated theoretically in predicting mean flow scaling. A milestone for the mean momentum scaling is the von Karman's velocity-defect law [3], i.e.

$$U_c - U = u_\tau g(y/R) \quad (1)$$

where U is the streamwise mean velocity; U_c is the mean centerline velocity; u_τ is the friction velocity (defined later) and g is an unknown scaling function depending only on the wall distance y (normalized with the half channel height or pipe radius R). Later, Millikan [4] developed a matching argument deriving the celebrated Prandtl-Karman log-law of (1). However, all theoretical accounts have been restricted to the scaling in an overlap region (typically for $y \leq 0.15$), without addressing the influence of geometries on more than 80% of the flow domain. Most efforts devoted for the whole domain description are empirical, such as Coles wake function [5], composite pade approximation [6, 7], with limited accuracy and unknown domain of applicability. A recent work by L'vov et al [8] achieves a noteworthy description of channel and pipe flows, but its outer flow description invoking a fitting function derived from simulation data does not distinguish channel and pipe. Thus, a theoretical derivation for the complete expression of function g is still missing, which is particularly important to resolve recent vivid debates on the universality of the mean velocity scaling in the canonical wall-bounded turbulent flows [9].

In this paper, we present a novel attempt which identifies a universal mechanism deriving the mean velocity scaling for canonical wall-bounded flows, based on a symmetry consideration of wall constraints. Most importantly, the theory suggests a universal bulk flow constant for channel and pipe. This is accomplished by introducing a length function whose calculation based on a variational argument yields a geometry

dependence (planar versus circular) with an integer scaling exponent (4 for a flat channel and 5 for a cylindrical pipe). The analysis enables a prediction of (1) valid in the entire flow domain, and the predicted mean velocity profiles are in excellent agreement with several dozen of recent, reliable experiments over a wide range of Re 's. The results also shed light on the debate between the log-law and power-law [10, 11] in favor of the former, and have applications to other boundary effects (such as roughness, compressibility, pressure gradient - studied by us but not addressed here).

We start with the fully developed incompressible turbulent channel flow, between two parallel plates of height $2R$, driven by a constant pressure gradient $f_p = -\frac{1}{\rho} \frac{\partial p}{\partial x}$ in the stream-wise x -direction. The flow develops a mean-velocity profile U , depending on wall-normal y -direction only. The mean momentum flux is described by the Reynolds averaged Navier-Stokes (RANS) equation, i.e.

$$\nu \partial_y U - \overline{u'v'} = \tau_p. \quad (2)$$

where $S \equiv \partial_y U$ is mean shear; $W \equiv -\overline{u'v'}$ denotes Reynolds stress which is unknown; $\tau_p = \int_0^r f_p dr' = u_\tau^2 r/R$ is the total stress with $r = R - y$, the distance to the centerline, and $u_\tau \equiv \sqrt{f_p R}$ is the friction velocity determined by the pressure force. Note that dimensionally, (2) has an alternative interpretation at the local position r : the pressure gradient force supplies the energy $\tau_p = f_p r$ which balances the viscous damp νS and the turbulent shear fluctuation W . In this sense, for a cubic flow volume in a channel, namely $V_r = r \times R \times R$ ($R \times R$ indicates the r -surface area), the total turbulent shear fluctuation energy is thus $M = \int_0^{V_r} W d\mathbf{v}$ (we will return to this quantity later).

Then, the product of viscous and Reynolds stresses contributes to the growth of the turbulent kinetic energy $k = \overline{u_i' u_i'}/2$, which is described by the mean kinetic energy equation, i.e.

$$S W + \Pi = \varepsilon. \quad (3)$$

Here $\mathcal{P} = S W$ is the production; Π represents the spatial energy transfer (including diffusion, convection and fluctuation transport); ε the viscous dissipation (for explicit expressions, see [12]).

In our recent work [13], a dimensional analysis among ε, S, W yields

$$\ell = W^{(\frac{1}{n} + \frac{1}{2})} S^{(\frac{1}{n} - 1)} \varepsilon^{(-\frac{1}{n})}, \quad (4)$$

where ℓ is the characteristic length representing eddies responsible for the energy spatial transfer, and n is an arbitrary real number, tentatively chosen to be integer. Note that as $n \rightarrow \infty$, the length becomes the classical mixing length of Prandtl: $\ell_\infty = \sqrt{W/S}$; while a unique $n = 4$ defines a physically meaningful length valid throughout the channel, i.e.

$$\ell_\varepsilon = W^{\frac{3}{4}} S^{-\frac{3}{4}} \varepsilon^{-\frac{1}{4}}. \quad (5)$$

This length is similar to the crucial scaling function in the model of L'vov et al. [8] (restricted to the bulk zone only), but its interpretation follows a concept of order function developed by us [14]. Our main result of this paper is to give a physical derivation of ℓ_ε .

According to its definition (5), ℓ_ε can also be expressed in terms of the eddy viscosity $\nu_t = W/S$, i.e. $\ell_\varepsilon = \nu_t^{3/4} / \varepsilon^{1/4}$. This expression reminds us of the Kolmogorov dissipation length $\eta = \nu^{3/4} / \varepsilon^{1/4}$, where ν is the kinematic viscosity. Following the interpretation of η , ℓ_ε is presumably related to turbulence production eddies (since $SW = P$), hence called the length of production eddies (PE). In analogy to Townsend [15], a possible materialization of PE is through the ensemble averaged vortex packets [16] or clusters [17]. Moreover, recalling the attached eddy hypothesis by Perry [18], we assume similarly that PE distribute uniformly in the spanwise direction (since time average is applied), and the streamwise characteristic size is ℓ_ε - only depending on centerline distance r . In figure 1, we depict the distribution of PE in a channel (and a pipe), where one can see a monotonic decrease of ℓ_ε away from centerline, indicating the influence of wall constraint $\ell_\varepsilon = 0$ approaching the wall. Note that one can also interpret the increment of ℓ_ε approaching the centerline as the growth of PE, in analogy to the growth of the wall attached eddies as wall distance increases [18]. Under such a statistical point of view, we will consider two important quantities associated with the PE, which are the total shear fluctuation energy M' (from Reynolds shear stress), and the total kinetic energy E' associated with the growth of PE, as presented below.

Recall that the total shear fluctuation energy for a given flow volume V_r is M . Then, for the shear fluctuation energy of PE sketched in figure 1, an volume integration of W yields $M' = \int_0^r W \ell_\varepsilon R dr = \int_0^{V_r} W(\ell_\varepsilon/R) d\mathbf{v}$. Moreover, as $\nabla \ell_\varepsilon$ represents the growth rate of PE size as y increases, and u_τ is a global velocity scale, thus $u_\tau \nabla \ell_\varepsilon$ represents the increment momentum due to the PE's growing size, and $E' = \int_0^{V_r} |u_\tau \nabla \ell_\varepsilon|^2 d\mathbf{v}$ is the total kinetic energy associated with the growth of PE.

Now, a variational argument is postulated by assuming that for a given M' (determined by the pressure force since $W \approx \tau_p$), E' should be minimum - as the flow reaches a quasi-equilibrium state. In other words, turbulent fluctuations dissipate kinetic energy, resulting in a minimum of E' for the

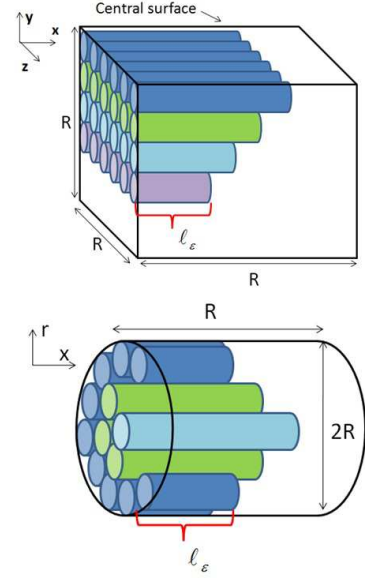


FIG. 1: Sketch of PE (tubes) with streamwise length scale ℓ_ε (depending on centerline distance) in a channel flow volume $V_R = R^3$ (left), and a pipe flow volume $V_R = \pi R^3$ (right).

growth of PE. As both M' and E' depend on ℓ_ε , following the calculus of variations [19], we thus require for all infinitesimal variations $\delta \ell_\varepsilon$,

$$\delta E' - \alpha \delta M' = 0, \quad (6)$$

where α is a dimensionless Lagrange multiplier. Generally, α depends on V_r since M' and E' are integrated over V_r . To nondimensionalize V_r , a simple choice is $\alpha = \alpha_0 V_r / V_R$, where α_0 is a constant and $V_R = R^3$ is the total cubic volume. It turns out that such a constant α_0 assumption is supported by the results shown later.

By substituting $\delta E' = -2 \int_0^{V_r} u_\tau^2 \Delta \ell_\varepsilon \delta \ell_\varepsilon d\mathbf{v}$ and $\delta M' = \int_0^{V_r} (W/R) \delta \ell_\varepsilon d\mathbf{v}$ into (6), we thus obtain a diffusion equation for ℓ_ε (eliminating the volume integral),

$$-2u_\tau^2 \Delta \ell_\varepsilon - \alpha W/R = 0. \quad (7)$$

With $W \approx \tau_p = u_\tau^2 r/R$, $\alpha = \alpha_0 V_r / R^3 = \alpha_0 r/R$, we have $2\Delta \ell_\varepsilon \approx -\alpha_0 r^2 / R^3$, which, after integrating with r , leads to $\ell_\varepsilon / R \approx -\alpha_0 (r/R)^4 / 24 + a_1 r/R + a_2$. Note that $a_1 = 0$ due to the central symmetry ($\partial_r \ell_\varepsilon = 0$ at $r = 0$), and $a_2 = \alpha_0 / 24$ due to the wall condition ($\ell_\varepsilon = 0$ at $r = R$). Therefore, ℓ_ε in a channel flow is:

$$\ell_\varepsilon^{CH} / R \approx \kappa (1 - r'^4) / 4 \quad (8)$$

where $\kappa = \alpha_0 / 6$ and $r' = r/R$ is substituted. (8) is validated in figure 2 using direct numerical simulation (DNS) data. It is clear that different Re 's profiles of ℓ_ε collapse and agree well with (8) almost in the entire flow domain. The only empirical parameter $\kappa \approx 0.45$ is extracted from DNS data, indicating $\alpha_0 = 6\kappa \approx 2.7$, a constant expected by the preceding analysis.

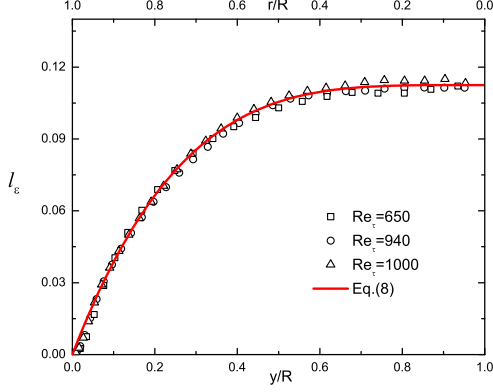


FIG. 2: Characteristic length $\ell_\epsilon = \ell_\infty/\Theta^{1/4}$ at different Re_τ 's in channels. Bottom axis is the wall distance y/R and the up axis is the centerline distance r/R . The curve (8) exhibits convincing data collapse with $\kappa = 0.45$. Symbols are DNS data of ℓ_∞^{DNS} divided by theoretical Θ with $r_c = 0.27$. Data are from Iwamoto *et al* [20] ($Re_\tau = 650$); Hoyas & Jimenez [21] ($Re_\tau = 940$); Lee & Moser [22] ($Re_\tau = 1000$).

All above analysis can be equally applied to turbulent pipe flow. The difference from channel is that, the flow volume corresponding to the cylindrical boundary (see figure 1) is $V_r = R\pi r^2$, and $M' = \int_0^r W \ell_\epsilon 2\pi r dr = \int_0^{V_r} W(\ell_\epsilon/R) dV$, $V_R = \pi R^3$. In this case, $\alpha = \alpha_0 r^2/R^2$, and a similar calculation of (7) for pipe flow yields

$$\ell_\epsilon^{Pipe}/R \approx \kappa(1 - r'^5)/5. \quad (9)$$

Here the coefficient $\kappa/5$ is determined by requiring the same near wall asymptotic scaling as (8), i.e. $\ell_\epsilon^{Pipe}/R \approx \ell_\epsilon^{CH}/R \approx \kappa(y/R)$ when $r' \rightarrow 1$. This is reasonable because the geometry effect vanishes close to the wall, hence channel and pipe should share the same κ (validated later). Also note that for turbulent boundary layer (TBL), though W may different from channel to TBL, a leading order expansion $W \propto r/R$ (r is the distance to the boundary layer thickness R) in TBL would also lead to (8) based on (7). In other words, (8) in channel should also apply in TBL when the latter flow becomes nearly parallel (at large Re 's); this result is in consistent with the same flat plate wall condition in the two flows.

Interestingly, a joint solution of (2) and (3) can be obtained using ℓ_ϵ and $\Theta = \varepsilon/(SW)$. From (5) one has $S = \sqrt{W}/(\ell_\epsilon \Theta^{1/4})$. Integrating S with r and using $W \approx \tau_p$, one obtains the velocity-defect law (1), i.e.

$$U_c - U = \int_0^r S d\hat{r} \approx \int_0^r \frac{\sqrt{\tau_p}}{\ell_\epsilon \Theta^{1/4}} d\hat{r} \quad (10)$$

Here $\Theta = [1 + (r_c/r')^2]/(1 + r_c^2)$ has been derived in [13]; it connects two asymptotes, i.e. $\Theta \rightarrow 1$ as $r' \rightarrow 1$ and $\Theta \rightarrow 1/r'^2$ as $r' \rightarrow 0$ smoothly, valid for the entire flow domain. Note that (10) also rewrites as

$$\kappa U_d/u_\tau = G(r') \approx \int_0^{r'} f(\hat{r}) d\hat{r}, \quad (11)$$

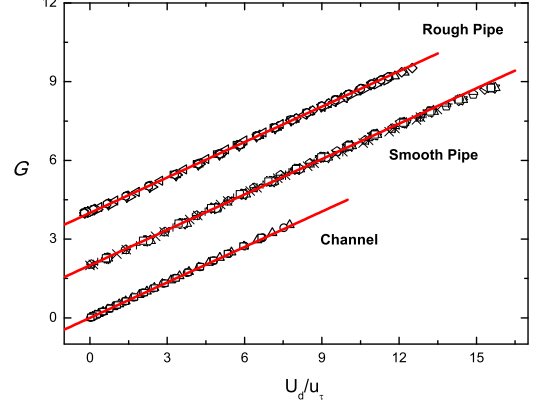


FIG. 3: Empirical U_d/u_τ versus theoretical scaling function G for 25 profiles in the bulk flow region ($50 \leq yu_\tau/\nu \leq Re_\tau$), elucidating a good linear relation with a universal slope $\kappa = 0.45$ (lines) in (11) for Re_τ varying over three decades. Profiles are vertically staggered for clarity. There are 3 profiles from DNS channel (data are the same as in figure 2); 14 profiles from Princeton smooth pipe with Re_τ from 6×10^3 to 5×10^5 [23] and 8 from rough pipe with Re_τ from 1×10^4 to 2×10^5 [24].

where $U_d = U_c - U$, $f = m[(1 + r_c^2)/(\hat{r}^2 + r_c^2)]^{1/4} \hat{r}/(1 - \hat{r}^m)$ ($m = 4$ for channel and 5 for pipe). The parameter r_c indicates the thickness of the core layer in channel and pipe (zero in TBL due to the absence of opposite wall), which has a slight Re -dependence at moderate Re 's. It is obtained by fitting G with the velocity-defect data, which yields $r_c \approx 0.27$ for channels (DNS) and $r_c \approx 0.5$ for Princeton pipes (EXP). The predicted velocity defect is shown in figure 3, where the universal bulk flow constant $\kappa \approx 0.45$ is remarked by the linear slope agreeing well with 25 sets of mean velocity profiles. Note that the result for smooth pipe is also applied to rough pipe (with the same κ and r_c), consistent with the Townsend's similarity hypothesis [15].

It is important to note that our current results support the asymptotic log-law instead of power-law. Note that at large Re 's, there would be an asymptotic interval where $\Theta \approx 1$, $\tau_p \approx u_\tau^2$ and $\ell_\epsilon \approx \kappa y$. In this region, $\ell_\epsilon \approx \ell_\infty$, so the present calculation is identical to the Prandtl-Karman's log-law [1, 12], $\ell_\infty \approx \kappa_K y$. This implies that the bulk flow constant κ derived in the present study is exactly the Karman constant κ_K . Furthermore, rewriting (11) as $U/u_\tau = U_c/u_\tau - G/\kappa$, and the leading order contribution in G is $\int_0^{1-y/R} 1/(1-\hat{r}) d\hat{r} \propto \ln(y/R)$, we thus have $U/u_\tau - U_c/u_\tau \propto \kappa^{-1} \ln(y/R)$, indicating the logarithmic scaling. Thus our results support the asymptotic log-law. In figure 4, using the empirical U_c (and κ , r_c), we plot the mean velocity by (11), displaying impressive agreement with data (smooth and rough pipes only; channel data also agree well, but not shown). The relative errors are bounded within 1% (except for first several points near wall) - the same level as the data uncertainty. Note that the inner bound of (11) reaches as close to the wall as $yu_\tau/\nu \approx 50$ (buffer layer thickness).

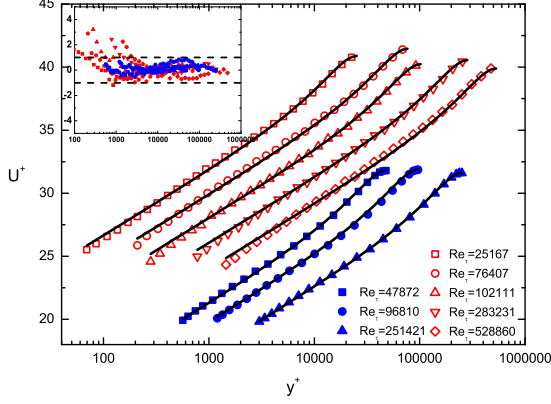


FIG. 4: Mean velocity data (symbols) compared with (11) (lines), using empirical U_c/u_τ , κ and r_c . Open symbols indicate smooth pipes [23] while solids indicate rough pipes [24]. Inset shows relative errors (times 100) which are mostly bounded within 1% (dashed lines). Profiles for smooth pipes are vertically staggered for clarity.

The correction within the buffer layer needs wall function, to be reported elsewhere.

Finally, the dissipation and transport in the mean kinetic energy equation (3) are predicted:

$$\begin{aligned} \varepsilon &= SW\Theta \approx \frac{u_\tau^3}{R} \frac{m(r'^2 + r_c^2)^{3/4}}{\kappa(1 - r'^m)(1 + r_c^2)^{3/4}} \\ \Pi &= SW(\Theta - 1) \approx \frac{u_\tau^3}{R} \frac{mr_c^2(1 - r'^2)(r'^2 + r_c^2)^{-1/4}}{\kappa(1 - r'^m)(1 + r_c^2)^{3/4}} \end{aligned} \quad (12)$$

Particularly, the centerline dissipation (equaling centerline transport) is:

$$\varepsilon_0 = \Pi_0 \approx \frac{u_\tau^3}{R} \frac{mr_c^{3/2}}{\kappa(1 + r_c^2)^{3/4}} \quad (13)$$

With the value $\kappa \approx 0.45$ and $r_c \approx 0.5$, we have $\varepsilon_0 \approx 3.3u_\tau^3/R$ for pipe. For current channel data, using $\kappa \approx 0.45$ and $r_c \approx 0.27$ yields $\varepsilon_0 \approx 1.2u_\tau^3/R$. However, since r_c has a moderate Re -effect (indicating a growth of central core layer), the predicted centerline dissipation may increase with increasing Re . Assuming the same r_c for high Re channels and pipes, one would have $\varepsilon_0^{Pipe}/\varepsilon_0^{CH} = 5/4$. These await verifications when ε_0 data are available.

In summary, we have developed an analytical theory for joint closures of the mean momentum and kinetic energy equations for turbulent channel and pipe flows. The variational assumption leads to an analytical formula of the eddy length function, where a universal bulk flow constant $\kappa \approx 0.45$

is identified to be valid for the entire flow domain (much beyond the overlap region). Note that (8) and (9) indicate a breaking of dilation invariance for ℓ_ε because of the presence of a characteristic length $\ell_0 = \kappa R/m$ at the centreline. However, the dilation invariance is preserved in its gradient, i.e. $d\ell_\varepsilon/dr' \propto r'^{m-1}$. Such a symmetry perspective is further explored in connection of the dilation symmetry in the direction normal to the wall for turbulence model equations widely used in engineering applications (i.e. $k - \omega$ equation), which will be reported elsewhere.

This work is supported by National Nature Science (China) Fund 11452002 and 11521091 and by MOST (China) 973 project 2009CB724100.

* Electronic address: she@pku.edu.cn

- [1] P. A. Davidson, et al., 2011 *A voyage through turbulence*. Cambridge University Press.
- [2] A.J. Smits & I. Marusic, *Physics Today*, 66(9), 25 (2013).
- [3] T. von Kármán, *Proc. Trird Int. Congr. Applied Mechanics*, Stockholm, 85-105 (1930).
- [4] C. B. Millikan, In *Proceedings 5th International Congress on Applied Mechanics*. Cambridge, MA 386-392 (1938).
- [5] D. Coles, *Journal of Fluid Mechanics*. 1(02) 191-226 (1956).
- [6] P. A. Monkewitz, et al., *Phys. Fluids*. 19, 115101 (2007).
- [7] H. M. Nagib, & K. A. Chauhan, *Phys. Fluids*. 20, 101518 (2008).
- [8] V.S. L'vov, et al., *Phys. Rev. Lett.* 100, 050504 (2008).
- [9] I. Marusic, et al., *Phys. Fluids*. 22, 065103 (2010).
- [10] G.I. Barenblatt & A.J. Chorin, *Proc. Natl Acad. Sci. USA* 101, 15023-15026 (2004).
- [11] W. K. George, *AIAA Journal*, 44(11), 2435-2449 (2006).
- [12] P.A. Davidson, *Turbulence: An Introduction for Scientists and Engineers*. (Oxford University Press, 2004).
- [13] X. Chen & Z.S. She, arXiv:1604.08257, (2016).
- [14] Z.S. She, et al., *Acta Mechanica Sinica* 26 (6), 847-861 (2010).
- [15] A.A. Townsend, 1976 *The strucutre of turbulent shear flow*. Cambridge University Press.
- [16] R.J. Adrian, *Phys. Fluids*. 19, 041301 (2007).
- [17] J. Jimenez, *Annu. Rev. Fluid Mech.* 44, 27-45 (2012).
- [18] A.E. Perry & M.S. Chong, *Journal of Fluid Mechanics*. 119, 173-217 (1982).
- [19] F.P. Bretherton & D. B. Haidvogel, *Journal of Fluid Mechanics*. 78(01) 129-154 (1976).
- [20] Iwamoto, K., Suzuki, Y., Kasagi, N., THTLAB Internal Report. No. ILR-0201 (2002).
- [21] Hoyas, S., Jimenez, J., *Phys. Fluids*. 18, 011702 (2006).
- [22] M. Lee & R. D. Moser, *Journal of Fluid Mechanics*. 774, 395-415 (2015).
- [23] B. J. McKeon, et al., *Journal of Fluid Mechanics*, 501, 135-147 (2004).
- [24] M.A. Schockling, et al., *Journal of Fluid Mechanics*, 564, 267-285 (2006).